

Ultracold collisions between two light indistinguishable diatomic molecules: elastic and rotational energy transfer in HD+HD

Renat A. Sultanov^{*,1,2} Dennis Guster^{†,2} and S. K. Adhikari^{‡1}

¹*Instituto de Física Teórica, UNESP – Universidade Estadual Paulista, 01140 São Paulo, SP, Brazil*

²*Department of Information Systems and BCRL,
St. Cloud State University, St. Cloud, MN, USA*

(Dated: September 19, 2018)

A close coupling quantum-mechanical calculation is performed for rotational energy transfer in a HD+HD collision at very low energy, down to the ultracold temperatures: $T \sim 10^{-8}$ K. A global six-dimensional $\text{H}_2\text{-H}_2$ potential energy surface is adopted from a previous work [Boothroyd *et al.*, *J. Chem. Phys.*, **116**, 666 (2002).] State-resolved integral cross sections $\sigma_{ij \rightarrow i'j'}(\epsilon_{kin})$ of different quantum-mechanical rotational transitions $ij \rightarrow i'j'$ in the HD molecules and corresponding state-resolved thermal rate coefficients $k_{ij \rightarrow i'j'}(T)$ have been computed. Additionally, for comparison, H_2+H_2 calculations for a few selected rotational transitions have also been performed. The hydrogen and deuterated hydrogen molecules are treated as rigid rotors in this work. A pronounced isotope effect is identified in the cross sections of these collisions at low and ultracold temperatures.

PACS numbers: 34.50.Cx 34.50.Ez

I. INTRODUCTION

The recent creation and investigation of a quantum gas of ultracold diatomic molecules [1] is of great interest in many areas of atomic, molecular, optical, and chemical physics [2–6]. Research in these fields may have important future applications, for example, in quantum information processing [7–10]. From a scientific point of view the creation of the molecular quantum gas opens new doors, for instance, in the experimental and theoretical investigation of the cold and ultracold molecular scattering and chemical reactions [11–16]. It allows researchers to probe the interaction and collisional properties of different light and heavy molecules in the cold and ultracold regime: $T \sim 10^{-4} - 10^{-8}$ K [5, 6, 11, 17, 18]. In this regime, one can expect many shape resonances in the cross sections arising from the van der Waals force [5, 6]. For example, a resonance with a weakly bound level near zero collision energy can significantly enhance the tunneling effect through a reaction barrier. By aligning and orienting the colliding molecules, the anisotropy of the van der Waals forces enables substantial tuning of the molecular levels to create such resonances [5].

In this work, the ultracold collision between two deuterated hydrogen molecules, i.e. rotational energy transfer in HD+HD, is mainly considered. For comparison similar collision in H_2+H_2 is also considered. From a theoretical point of view the HD+HD system is interesting because its PES can be derived from the much-studied H_2+H_2 system by adjusting the coordinate of the HD-molecule center of mass. Once the symmetry is broken in $\text{H}_2\text{-H}_2$ by replacing the H with a D atom in

each H_2 we have the precise HD-HD PES. The HD and H_2 molecules are treated as rigid monomer rotors in this work, so we ignore the vibrational degrees of freedom of these molecules.

Because of the small reduced mass and large rotational-energy spacing in the HD-HD system, the number of states required in the basis set for an accurate quantum-mechanical calculation should be relatively small. The HD+HD system has widely spaced rotational-energy levels and, because of the strong anisotropy of the intermolecular potential, it has relatively large rotational-energy transition probabilities. Since HD is a light molecule it can be manipulated easily by an external electrical field and also, the laser cooling of this diatomic molecule seems possible making this system is of current experimental interest.

Surprisingly, such a fundamental and attractive quantum four-atomic system has not received substantial attention in previous experimental and theoretical investigations. Several molecular-beam studies of HD+HD involve the measurement of a few rotational probabilities [19], integral cross sections for unresolved internal [20], and rotational energy transfer rates [21, 22]. Nevertheless, there are only a few calculations dealing with the rotational excitation in the HD+HD collision, e. g., an early modified-wave-number calculation by Takayanagi [23], semiclassical calculations by Gelb and Alper [24], and Cacciatore and Billing [25].

Hydrogen isotope effects have often attracted considerable attention [26]. In this work we carry out such consideration within the HD+HD and H_2+H_2 systems at high, low and ultracold temperatures. In the next section we briefly present the quantum-mechanical approach, that is used in this work and the PES. In Sec. III we present numerical results for both HD+HD and H_2+H_2 collisions. Additionally, we present a brief discussion of the numerical convergence of the results. Finally, in Sec. IV we present a summary and conclusion.

*rasultanov@stcloudstate.edu (r.sultanov2@yahoo.com)

†dcguster@stcloudstate.edu

‡adhikari@ift.unesp.br; http://www.ift.unesp.br/users/adhikari

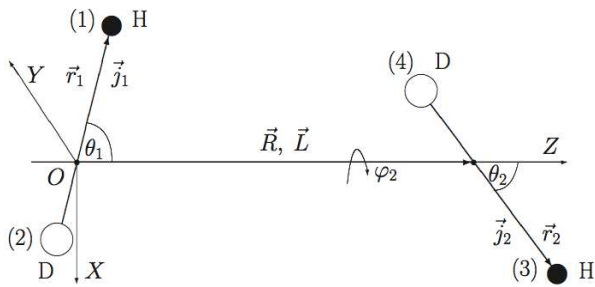


FIG. 1: Four-atomic system (12) + (34) or HD+HD, where H is a hydrogen atom and D is deuterium, represented by few-body Jacobi coordinates: \vec{r}_1 , \vec{r}_2 , and \vec{R} . The vector \vec{R} connects the center of masses of the two HD molecules and is directed over the axis OZ , θ_1 is the angle between \vec{r}_1 and \vec{R} , θ_2 is the angle between \vec{r}_2 and \vec{R} , φ_2 is the torsional angle, \vec{j}_1, \vec{j}_2 , and \vec{L} are quantum angular momenta over the corresponding Jacobi coordinates \vec{r}_1 , \vec{r}_2 , and \vec{R} .

II. METHOD: QUANTUM DYNAMICS

Here we briefly present the close-coupling quantum-mechanical approach used in this study to calculate the cross sections and thermal rate coefficients of molecular hydrogen-hydrogen collision. The Schrödinger equation for the (12) + (34) collision in the center of a mass frame, where (12) and (34) are linear rigid rotors is [27, 28]:

$$\left(\frac{P_{\vec{R}}^2}{2M_{12}} + \frac{L_{\hat{r}_1}^2}{2\mu_{1(2)}} + \frac{L_{\hat{r}_2}^2}{2\mu_{2(4)}} + V(\vec{r}_1, \vec{r}_2, \vec{R}) - E \right) \times \Psi(\hat{r}_1, \hat{r}_2, \vec{R}) = 0, \quad (1)$$

where $P_{\vec{R}}$ is the relative momentum operator, \vec{R} is the relative position vector, M_{12} is the reduced mass of the pair $M_{12} = (m_1 + m_2)(m_3 + m_4)/(m_1 + m_2 + m_3 + m_4)$, $\mu_{1(2)}$ are reduced masses of the targets: $\mu_{1(2)} = m_{1(3)}m_{2(4)}/(m_{1(3)} + m_{2(4)})$, $\hat{r}_{1(2)}$ are the angles of orientation of rotors (12) and (34), respectively, E is the total center-of-mass energy and $V(\vec{r}_1, \vec{r}_2, \vec{R})$ is the potential energy surface for the four atomic system (12) + (34). The system is shown in Fig. 1. Basically, the PESs of the H_2 - H_2 and the HD-HD systems are the same. However, there is a small but important difference. To obtain the HD-HD PES from the existing H_2 - H_2 surface [29] one needs to appropriately shift the center of mass in the hydrogen molecules (H_2). The usual rigid rotor model [27, 30–33] has also been applied in astrophysical calculations of different atom and diatomic-molecule collisions or two diatomic-molecule collisions at low temperatures: $T < 2000$ K.

The eigenfunctions of the operators $L_{\hat{r}_{1(2)}}$ in Eq. (1) are simple spherical harmonics $Y_{j_i m_i}(\hat{r})$. To solve Eq. (1)

the following expansion is used [27]:

$$\Psi(\hat{r}_1, \hat{r}_2, \vec{R}) = \sum_{JM j_1 j_2 j_{12} L} \frac{U_{j_1 j_2 j_{12} L}^{JM}(R)}{R} \times \phi_{j_1 j_2 j_{12} L}^{JM}(\hat{r}_1, \hat{r}_2, \vec{R}), \quad (2)$$

where J is the total angular momentum quantum number, M is its projection onto the space fixed z axis and the channel expansion functions are

$$\phi_{j_1 j_2 j_{12} L}^{JM}(\hat{r}_1, \hat{r}_2, \vec{R}) = \sum_{m_1 m_2 m_{12} m} C_{j_1 m_1 j_2 m_2}^{j_{12} m_{12}} C_{j_{12} m_{12} L m}^{JM} \times Y_{j_1 m_1}(\hat{r}_1) Y_{j_2 m_2}(\hat{r}_2) Y_{L m}(\hat{R}), \quad (3)$$

with $j_1 + j_2 = j_{12}$, $j_{12} + L = J$, m_1, m_2, m_{12} and m are the projections of j_1, j_2, j_{12} and L respectively.

Substitution of Eq. (2) into (1) provides a set of coupled second order differential equations for the unknown radial functions $U_{\alpha}^{JM}(R)$

$$\left(\frac{d^2}{dR^2} - \frac{L(L+1)}{R^2} + k_{\alpha}^2 \right) U_{\alpha}^{JM}(R) = 2M_{12} \sum_{\alpha'} \int \langle \phi_{\alpha}^{JM}(\hat{r}_1, \hat{r}_2, \vec{R}) | V(\vec{r}_1, \vec{r}_2, \vec{R}) | \phi_{\alpha'}^{JM}(\hat{r}_1, \hat{r}_2, \vec{R}) \rangle U_{\alpha'}^{JM}(R) d\hat{r}_1 d\hat{r}_2 d\hat{R}, \quad (4)$$

where $\alpha \equiv (j_1 j_2 j_{12} L)$. We apply the hybrid modified log-derivative-Airy propagator in the general purpose scattering program MOLSCAT [34] to solve the coupled Eqs. (4). Additionally, we have tested other propagator schemes included in MOLSCAT. Our calculations revealed that other propagators can also produce quite stable results.

Boothroyd *et al.* (BMKP) [29] constructed a global six-dimensional PES for two hydrogen molecules, especially to represent the whole interaction region of the chemical reaction dynamics of the four-atomic system and to provide an accurate estimate of the van der Waals well. The ground state and a few excited-state energies were calculated. In the six-dimensional configuration space of the H_2 - H_2 system the conical intersection forms a complicated three-dimensional hyper surface. The new potential fits the van der Waals well to an accuracy of about 5% [29]. In our calculation of the BMKP PES for H_2 + H_2 the bond length was fixed at 1.449 a.u. or $r(H_2)=0.7668$ Å as in the Diep and Johnson (DJ) PES [35]. In the case of the HD+HD calculation the bond length of HD was adopted at $r(HD) = 0.7631$ Å.

The log-derivative matrix of the wave function is propagated to large R -intermolecular distances, since all experimentally observable quantum information about the collision is contained in the asymptotic behavior of functions $U_{\alpha}^{JM}(R \rightarrow \infty)$. The numerical results are matched to the known asymptotic solution to derive the physical

scattering S -matrix

$$U_{\alpha}^J \underset{R \rightarrow +\infty}{\sim} \delta_{\alpha\alpha'} e^{-i(k_{\alpha\alpha} R - (l\pi/2))} - \left(\frac{k_{\alpha\alpha}}{k_{\alpha\alpha'}}\right)^{1/2} S_{\alpha\alpha'}^J \times e^{-i(k_{\alpha\alpha'} R - (l'\pi/2))}, \quad (5)$$

where $k_{\alpha\alpha'} = [2M_{12}(E + E_{\alpha} - E_{\alpha'})]^{1/2}$ is the channel wave number, $E_{\alpha(\alpha')}$ are rotational channel energies and E is the total energy in the (1234) system. The method was used for each partial wave until a converged cross section was obtained.

Cross sections for rotational excitation and relaxation can be obtained directly from the S -matrix. In particular the cross sections for excitation from $j_1 j_2 \rightarrow j'_1 j'_2$ summed over the final $m'_1 m'_2$ and averaged over the initial $m_1 m_2$ are given by

$$\sigma(j'_1, j'_2; j_1 j_2, \varepsilon) = \sum_{J j_{12} j'_{12} L L'} \frac{\pi(2J+1)}{(2j_1+1)(2j_2+1)k_{\alpha\alpha'}} \times |\delta_{\alpha\alpha'} - S^J(j'_1, j'_2, j'_{12} L'; j_1, j_2, j_{12}, L; E)|^2. \quad (6)$$

The kinetic energy is $\varepsilon = E - B_1 j_1(j_1+1) - B_2 j_2(j_2+1)$, where $B_{1(2)}$ are the rotation constants of rigid rotors (12) and (34) respectively.

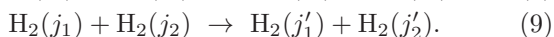
The relationship between the rate coefficient $k_{j_1 j_2 \rightarrow j'_1 j'_2}(T)$ and the corresponding cross section $\sigma_{j_1 j_2 \rightarrow j'_1 j'_2}(\varepsilon)$ can be obtained through the following weighted average

$$k_{j_1 j_2 \rightarrow j'_1 j'_2}(T) = \sqrt{\frac{8k_B T}{\pi\mu}} \frac{1}{(k_B T)^2} \int_{\varepsilon_s}^{\infty} \sigma_{j_1 j_2 \rightarrow j'_1 j'_2}(\varepsilon) \times e^{-\varepsilon/k_B T} \varepsilon d\varepsilon, \quad (7)$$

where k_B is Boltzmann constant, μ is reduced mass of the molecule-molecule system and ε_s is the minimum kinetic energy for the levels j_1 and j_2 to become accessible.

III. RESULTS

In this section our numerical results for rotational transitions in HD+HD collision and *para/para*-hydrogen molecules are presented. We carry out state-to-state comparison between these two collisions for selected rotational transitions in the HD and H₂ molecules. Specifically the following rotational energy transfer processes are considered:



At first look one might expect that the scattering outputs of these two collisions (8) and (9) should be close to each other. This is because the PESs of H₂-H₂ and HD-HD are almost the same six-dimensional functions of the H₄ four-atomic system coordinates. This fact follows from the general idea of the Born-Oppenheimer

model [36] and simple theoretical atom-molecular consideration. Therefore, the two processes (8) and (9) should lead to similar results. At the same time the HD and H₂ molecules have different rotational constants. This difference is not dramatic: the rotational constant of H₂ is $B_e(\text{H}_2) = 60.8 \text{ cm}^{-1}$, but the same parameter for HD is $B_e(\text{HD}) = 44.7 \text{ cm}^{-1}$.

The HD+HD system has only four electrons. Further, the HD molecule consists of two nonidentical atoms which are in a covalent bond. In covalent bonding the spins of the electrons are antiparallel. The interaction of one of the nuclei, H⁺ or D⁺, with its own electron leads to a quantum configuration where the spin of its electron is oriented antiparallel to the spin of the nucleus, i.e. H⁺ or D⁺. Thus, the spins of H⁺ and D⁺ are antiparallel. Because the spin of H⁺ is $I_1 = -1/2$ and the spin of D⁺ is $I_2 = 1$ the resulting spin of the HD molecule nucleus is $I_{12} = 1/2$. This value has been adopted in the current calculation, although there may be other possible values. The processes (8) and (9) are collisions between two indistinguishable diatomic molecules. This fact is taken into account in this computation.

A. Comparison between HD+HD and H₂+H₂ state-selected integral cross sections

The precise HD-HD PES can be derived from the H₂-H₂ surface by adjusting, i.e. shifting, the coordinates of the center of masses of the two H₂ molecules to the center of masses of the HD molecules. Once the symmetry is broken in H₂-H₂ by replacing the H atoms with the D atoms in the two H₂ molecules we obtain the full HD-HD PES. The new potential will possess all parts of the HD-HD interaction. Therefore, it will be interesting to consider scattering in two systems, which are not very different like HD+HD and H₂+H₂.

In this work a large number of test calculations have been done to secure the convergence of the results with respect to all parameters that enter into the propagation of the Schrödinger equation (1). This includes the intermolecular distance R , the total angular momentum J of the four atomic system, the number of rotational levels N_{lvl} to be included in the close coupling expansion and some others, see the MOLSCAT manual [34]. We reached convergence for the integral cross sections, $\sigma(E_{kin})$, in all cases. However, it was particularly difficult to achieve convergence on the parameter R in both cases. For the applied BMKP PES we used $R_{min} = 2 \text{ \AA}$ to $R_{max} = 50 \text{ \AA}$. We also applied a few different propagators included in the MOLSCAT program.

In a previous paper we presented a detailed description of convergence test for H₂+H₂ collision [32]. The same numerical convergence has been achieved in this work. Namely, stable total cross sections have been obtained with respect to the number N_{lvl} of the rotational levels to be included in the basis set (2) of HD+HD, i. e., in each HD molecule the discrete integer quantum numbers

TABLE I: Rotational channel energies in the two hydrogen systems: a). HD + HD and b). *para*-H₂ + *para*-H₂

a). HD(j_1)+HD(j_2)					b). <i>para</i> -H ₂ (j_1)+ <i>para</i> -H ₂ (j_2)				
j_1	j_2	j_{12}	ν_a	$\epsilon_{j_1 j_2}^{HD}(\nu_a), \text{cm}^{-1}$	j_1	j_2	j_{12}	ν_b	$\epsilon_{j_1 j_2}^{H_2}(\nu_b), \text{cm}^{-1}$
0	0	0	1	0.0	0	0	0	1	0.0
0	1	1	2	89.4	0	2	2	2	364.8
0	2	2	3	268.2	0	4	4	3	1216.0
1	1	0	4	178.8	2	2	0	4	729.6
1	1	1	4	178.8	2	2	1	4	729.6
1	1	2	4	178.8	2	2	2	4	729.6
					2	2	3	4	729.6
					2	2	4	4	729.6
1	2	1	5	357.6	2	4	2	5	1580.8
1	2	2	5	357.6	2	4	3	5	1580.8
1	2	3	5	357.6	2	4	4	5	1580.8
					2	4	5	5	1580.8
					2	4	6	5	1580.8
2	2	0	6	536.4	4	4	0	6	2432.0
2	2	1	6	536.4	4	4	1	6	2432.0
2	2	2	6	536.4	4	4	2	6	2432.0
2	2	3	6	536.4	4	4	3	6	2432.0
2	2	4	6	536.4	4	4	4	6	2432.0
					4	4	5	6	2432.0
					4	4	6	6	2432.0
					4	4	7	6	2432.0
					4	4	8	6	2432.0

TABLE II: Comparison between different but “corresponding” ($\nu_a = \nu_b$) state-resolved cross-sections (\AA^2) in the HD + HD and *para*-H₂ + *para*-H₂ collisions at ultracold $T = 1.439 \cdot 10^{-8}$ K and very high $T = 14390.0$ K temperatures.

E_{kin}, K	HD(j_1)+HD(j_2) \rightarrow HD(j'_1) + HD(j'_2)						H ₂ (j_1) + H ₂ (j_2) \rightarrow H ₂ (j'_1) + H ₂ (j'_2)					
	$\epsilon_{j_1 j_2}^{HD}(\nu)$	j_1	j_2	j'_1	j'_2	$\sigma_{j_1 j_2 \rightarrow j'_1 j'_2}^{HD}$	$\epsilon_{j_1 j_2}^{H_2}(\nu)$	j_1	j_2	j'_1	j'_2	$\sigma_{j_1 j_2 \rightarrow j'_1 j'_2}^{H_2}$
1.439×10^{-8}	89.4	0	1	0	0	1.00×10^5	364.8	0	2	0	0	0.65×10^2
		0	0	0	1	3.34×10^{-5}		0	0	0	2	0.89×10^{-8}
	178.8	1	1	0	1	1.94×10^4	729.6	2	2	0	2	2.06×10^2
		1	1	0	0	0.50×10^4		2	2	0	0	17.8
	536.4	2	2	1	1	0.52×10^4	2432.0	4	4	2	2	2.31
		2	2	0	2	0.55×10^3		4	4	0	4	1.12
		2	2	0	1	0.94×10^3		4	4	0	2	0.50×10^{-1}
		2	2	0	0	1.28×10^2		4	4	0	0	1.94×10^{-3}
1.439×10^4	89.4	0	1	0	0	0.60	364.8	0	2	0	0	0.25
		0	0	0	1	1.78		0	0	0	2	1.18
	357.6	1	2	1	1	1.07	1580.8	2	4	2	2	0.44
		1	2	0	2	0.57		2	4	0	4	0.374

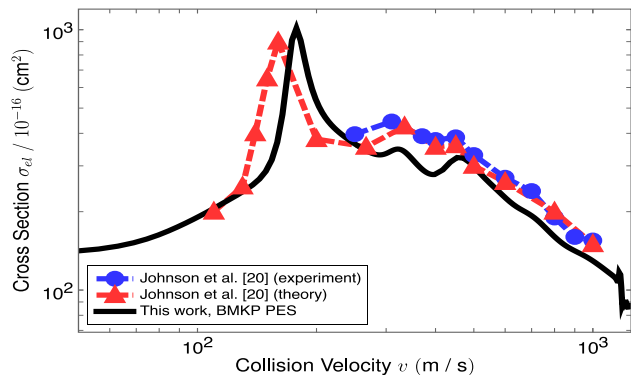


FIG. 2: (Color online) Integral cross sections for the HD+HD elastic scattering computed with the modified BMKP PES [29] together with the experimental and theoretical data from work [20].

j_1 and j_2 run from 0 to 4. As a result a maximum number $N_{lvl}(= 55)$ of rotational levels in HD+HD has been generated. With regard to the total quantum angular momentum J in the HD+HD system at $T \sim 10^{-8} - 10^{-6}$ K we needed to adopt just a few discrete values of this parameter, that is $J_{max} = 3$ or 4 was quite enough. However, at larger collision energies E_{kin} , such as, the ones we considered at $T \sim 4000$ K, one needs up to $J_{max} \approx 60$. In the case of $E_{kin} \sim 14000$ K: $J_{max} \approx 120$.

We present in Table I the rotational channel energies in the HD–HD and para-H₂–para-H₂ systems. This is a comparative table of the rotational spectra of these two systems. The first five columns from the left present HD–HD and the other five columns present the para-H₂–para-H₂ system; j_1 and j_2 are the quantum orbital momenta of the HD and H₂ molecules, $\vec{j}_{12} = \vec{j}_1 + \vec{j}_2$, with $|j_1 - j_2| \leq j_{12} \leq j_1 + j_2$, the index $\nu_{a(b)}$ is the current number of the degenerate rotational levels in HD and H₂, respectively. The rotational energy levels are shown in cm^{-1} . The goal of this work is to investigate the ultracold regime in HD+HD, calculate its rotational energy transfer cross sections and thermal rate coefficients, and to carry out comparison with the corresponding (when $\nu_a = \nu_b$, see Table I) rotational transitions in para-H₂–para-H₂ collision.

There are two slightly different definitions [37] of the rotational cross sections in collisions between two identical diatomic molecules, for example, in $\text{HD}(j_1) + \text{HD}(j_2) \rightarrow \text{HD}(j'_1) + \text{HD}(j'_2)$. The cross section for the rotational transition $j_1 j_2 \rightarrow j'_1 j'_2$ is [27, 34]: $\sigma \sim (1 + \delta_{j_1 j_2})(1 + \delta_{j'_1 j'_2})$. However, in Ref. [38] the same cross section has been defined as $\sigma \sim (1 + \delta_{j_1 j_2} \delta_{j'_1 j'_2})$. It is seen that the two cross sections coincide when $j_1 \neq j_2$ and $j'_1 \neq j'_2$. However, for other combinations of the rotational quantum numbers, namely, when $j_1 = j_2$ and/or $j'_1 = j'_2$, the cross section calculated in accord with Refs. [27, 34] is two times larger than the cross section from Ref. [38]. This has been taken into account in calculation

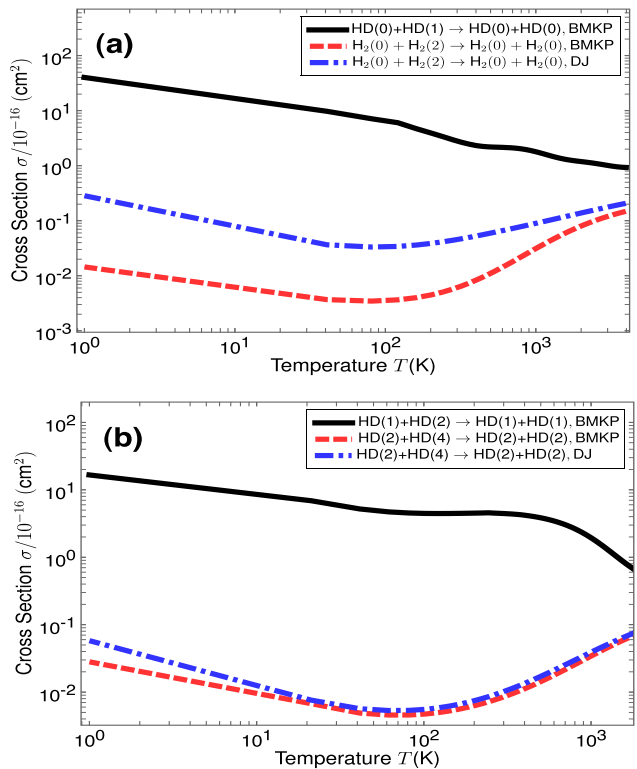


FIG. 3: (Color online) (a) Inelastic scattering integral cross sections for $\text{HD}(0) + \text{HD}(1) \rightarrow \text{HD}(0) + \text{HD}(0)$ and $\text{H}_2(0) + \text{H}_2(2) \rightarrow \text{H}_2(0) + \text{H}_2(0)$. (b) The same for $\text{HD}(1) + \text{HD}(2) \rightarrow \text{HD}(1) + \text{HD}(1)$ and $\text{H}_2(2) + \text{H}_2(4) \rightarrow \text{H}_2(2) + \text{H}_2(2)$.

with the MOLSCAT program [34], i.e., for the integral cross sections $\sigma(j'_1 j'_2; j_1 j_2, \epsilon)$ from Eq. (6) the following pre-factor $[(1 + \delta_{j_1 j_2})(1 + \delta_{j'_1 j'_2})]^{-1}$ has been adopted.

First, let us turn to HD+HD elastic scattering. In Fig. 2 we show results of this work computed with the modified BMKP PES [29] together with the corresponding data (experiment/theory) from relatively old papers [20]. As can be seen all these cross sections are in a satisfactory agreement with each other. This test calculation reveals the reliability of the modified BMKP PES, the computer program and the numerical convergence. One can see that at low and very low energies the general forms of the cross sections are rather close to each other with the exception of a shape resonance and small oscillations in the cross sections in Fig. 2.

In Table II few selected state-to-state cross sections for the HD+HD and H₂+H₂ collisions are presented. Here we compare results for few specific rotational excitation and de-excitation integral cross sections at only two values of kinetic energy, namely at $T_1 \sim 10^{-8}$ K, and at very high collision energy, i.e. $T_2 \sim 14,000$ K. At low temperature the HD+HD cross section could be larger by three to four orders of magnitude, whereas at high temperature the two cross sections are of the same order.

In Figs. 3, 4 and 5 we present a few state-selected

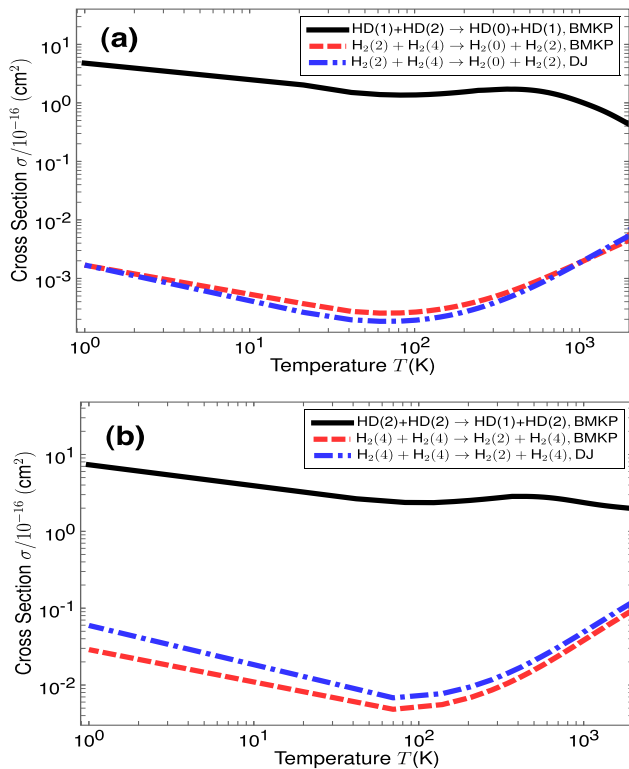


FIG. 4: (Color online) (a) Inelastic scattering integral cross sections for $\text{HD}(1) + \text{HD}(2) \rightarrow \text{HD}(0) + \text{HD}(1)$ and $\text{H}_2(2) + \text{H}_2(4) \rightarrow \text{H}_2(0) + \text{H}_2(2)$. (b) The same for $\text{HD}(2) + \text{HD}(2) \rightarrow \text{HD}(1) + \text{HD}(2)$ and $\text{H}_2(4) + \text{H}_2(4) \rightarrow \text{H}_2(2) + \text{H}_2(4)$.

rotational transition cross sections in collisions (8) and (9). It is useful to see the corresponding cross sections together on a single plot, that is when $\nu_a = \nu_b$. For example, in Fig. 3 (a) we show rotational transition de-excitation cross sections from the first excited states of HD and H_2 molecules, i.e. we consider $\text{HD}(0) + \text{HD}(1) \rightarrow \text{HD}(0) + \text{HD}(0)$ and $\text{H}_2(0) + \text{H}_2(2) \rightarrow \text{H}_2(0) + \text{H}_2(0)$ for a wide range of kinetic energies: from 1 K to up to 4000 K. In the case of $\text{H}_2 + \text{H}_2$, we carry out computations with two different PESs, e.g., with the BMKP PES [29] and with the Diep-Johnson (DJ) $\text{H}_2\text{-H}_2$ PES from Ref. [35]. The last one was formulated for fixed equilibrium distances between the hydrogen atoms in each H_2 molecule. In Fig. 3 (b) we show cross sections for some other de-excitation processes in the HD-HD system.

Further results for the integral cross section are shown in Figs. 4 and 5. The cross sections for following processes are presented in Fig. 4 (a): $\text{HD}(1) + \text{HD}(2) \rightarrow \text{HD}(0) + \text{HD}(1)$ and $\text{H}_2(2) + \text{H}_2(4) \rightarrow \text{H}_2(0) + \text{H}_2(2)$. The cross sections of $\text{HD}(2) + \text{HD}(2) \rightarrow \text{HD}(1) + \text{HD}(2)$ and $\text{H}_2(4) + \text{H}_2(4) \rightarrow \text{H}_2(2) + \text{H}_2(4)$ are shown in Fig. 4 (b). It is seen in Fig. 4 (a) that the HD+HD de-excitation cross sections could be larger than the $\text{H}_2 + \text{H}_2$ de-excitation cross sections by four orders of magnitudes. For the cross sections in Fig. 4 (b) the difference is about

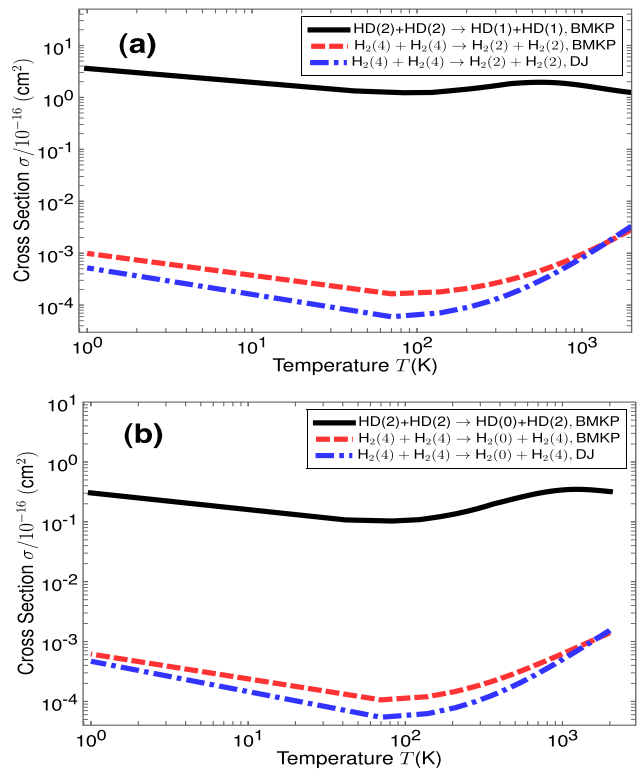


FIG. 5: (Color online) (a) Inelastic scattering integral cross sections for $\text{HD}(2) + \text{HD}(2) \rightarrow \text{HD}(1) + \text{HD}(1)$ and $\text{H}_2(4) + \text{H}_2(4) \rightarrow \text{H}_2(2) + \text{H}_2(2)$. (b) The same for $\text{HD}(2) + \text{HD}(2) \rightarrow \text{HD}(0) + \text{HD}(2)$ and $\text{H}_2(4) + \text{H}_2(4) \rightarrow \text{H}_2(0) + \text{H}_2(4)$.

a factor of 10^3 . In Fig. 5 (a) we show results for rotational transitions: $\text{HD}(2) + \text{HD}(2) \rightarrow \text{HD}(1) + \text{HD}(1)$ and $\text{H}_2(4) + \text{H}_2(4) \rightarrow \text{H}_2(2) + \text{H}_2(2)$. In Fig. 5 (b), we show the same for the following transitions. $\text{HD}(2) + \text{HD}(2) \rightarrow \text{HD}(0) + \text{HD}(2)$ and $\text{H}_2(4) + \text{H}_2(4) \rightarrow \text{H}_2(0) + \text{H}_2(4)$. Again, in both cases the HD+HD cross sections could be larger than the $\text{H}_2 + \text{H}_2$ at 1 K by four orders of magnitudes. We see in Figs. 3, 4, and 5 that, for the de-excitation processes for $\text{H}_2 + \text{H}_2$, the BMKP and the DJ PESs provide similar results with the exceptions shown in Fig. 2.

In Ref. [39] it was shown that for a specific excitation rotational transition in the $\text{H}_2 + \text{H}_2$ inelastic scattering, e.g., in $\text{H}_2(0) + \text{H}_2(0) \rightarrow \text{H}_2(0) + \text{H}_2(2)$, the BMKP PES provides an incorrect cross section when compared to the DJ potential. The comparison was also carried out with available experimental data [40]. Nevertheless, the BMKP PES has been applied to the important (astrophysical) *o*-/*p*- $\text{H}_2 + \text{HD}$ inelastic scattering problem [41, 42]. This is why we applied the BMKP PES to the HD+HD scattering problem.

In conclusion, based on the Born-Oppenheimer model treatment, the HD+HD and $\text{H}_2 + \text{H}_2$ have similar PESs. However, in the case of the HD-HD system the original $\text{H}_2\text{-H}_2$ PES is adopted and the two center of masses

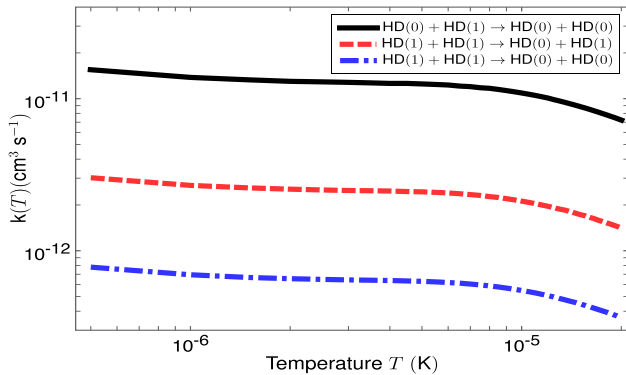


FIG. 6: (Color online) Thermal rate coefficients for the inelastic scattering processes: $\text{HD}(0) + \text{HD}(1) \rightarrow \text{HD}(0) + \text{HD}(0)$, $\text{HD}(1) + \text{HD}(1) \rightarrow \text{HD}(0) + \text{HD}(1)$, and $\text{HD}(1) + \text{HD}(1) \rightarrow \text{HD}(0) + \text{HD}(0)$, at ultracold temperatures.

of both H_2 molecules is just slightly shifted to the appropriate positions of the HD molecule center of masses. After this procedure we obtain the full space, i.e. global HD-HD PES. Our computations with this modified PES revealed a very strong isotopic effect in the HD+HD and H_2+H_2 collisions at low energies.

B. HD+HD rotational state-selected thermal rate coefficients at ultracold temperatures

We show in Figs. 6, 7, 8, and 9 the thermal rate coefficients in the inelastic HD+HD collision at very low temperatures from $\sim 5 \times 10^{-7}$ K to $\sim 2 \times 10^{-5}$ K. These results were obtained from corresponding state-resolved integral cross sections $\sigma_{j_1 j_2 \rightarrow j'_1 j'_2}(\epsilon)$ with the use of expression (7). Only de-excitation thermal rates have been computed, because at such a low temperature the excitation thermal rates are extremely small. The rates have

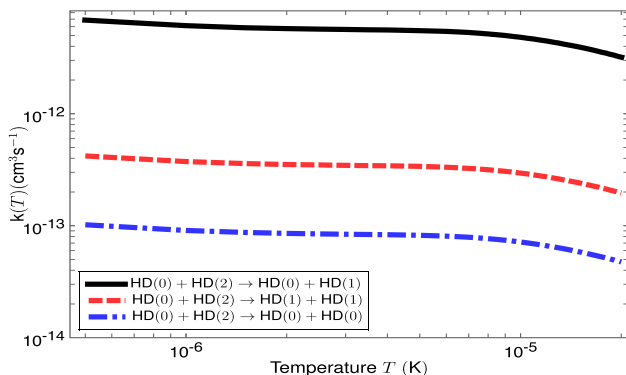


FIG. 7: (Color online) The same as in Fig. 6 for following processes: $\text{HD}(0) + \text{HD}(2) \rightarrow \text{HD}(0) + \text{HD}(1)$, $\text{HD}(0) + \text{HD}(2) \rightarrow \text{HD}(1) + \text{HD}(1)$, and $\text{HD}(0) + \text{HD}(2) \rightarrow \text{HD}(0) + \text{HD}(0)$.

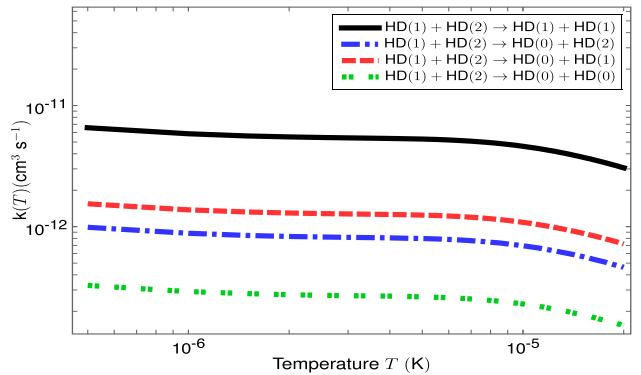


FIG. 8: (Color online) The same as in Fig. 6 for following processes: $\text{HD}(1) + \text{HD}(2) \rightarrow \text{HD}(1) + \text{HD}(1)$, $\text{HD}(1) + \text{HD}(2) \rightarrow \text{HD}(0) + \text{HD}(2)$, $\text{HD}(1) + \text{HD}(2) \rightarrow \text{HD}(0) + \text{HD}(1)$, and $\text{HD}(1) + \text{HD}(2) \rightarrow \text{HD}(0) + \text{HD}(0)$.

been computed for different initial rotational states of the HD molecules. The figure captions include the information about the specific state-selected rotational transitions in both HD molecules before and after collision.

In Fig. 6, we show results for the rates $k_{j_1 j_2 \rightarrow j'_1 j'_2}(T)$ for the inelastic scattering processes from the first three rotational states. In Fig. 7 we show the rates for transition from the excited states. These transitions correspond to different de-excitations from lower initial rotational states in the HD-HD system. In Fig. 6 the initial state for the solid line corresponds to the first excited rotational state in HD+HD. From Table I one can see that for this state of the system: $\nu_a=2$. The two other lines in Fig. 6 correspond to the initial state with $\nu_a=4$, i.e. $E_{in}=178.8 \text{ cm}^{-1}$. The rates for the initial state HD(1)+HD(1) in Fig. 6 are smaller than those for the initial state HD(0)+HD(1), although all three rates have similar dependence on temperature.

In Fig. 7 we show the rates for some de-excitation transitions from the initial state HD(0)+HD(2), which is the third rotational excited state in HD+HD: $\nu_a=3$. Although we again observe that the behavior of the thermal rates $k_{j_1 j_2 \rightarrow j'_1 j'_2}(T)$ is quite identical, their values significantly differ from each other, specifically up to two orders of magnitude. Further, the thermal rate coefficients $k_{j_1 j_2 \rightarrow j'_1 j'_2}(T)$ from the higher excited rotational states HD(1)+HD(2) and HD(2)+HD(2) are presented in Fig. 8 and 9, respectively. Specifically, these rates are from the energy levels 357.6 cm^{-1} and 536.4 cm^{-1} corresponding to the following two indices: $\nu_a=5$ and $\nu_a=6$, respectively (see Table I). In these calculations we needed a fairly extended number of basis functions in the expansion (2) for convergence. However, this is quite understandable because of the large energy of the initial state. For example, in the calculation of rotational transitions from that level with the following rotational indices $j_1 = 2, j_2 = 2$, i.e. $\nu_a = 6$ and $\epsilon_{j_1 j_2}^{HD} = 536.4 \text{ cm}^{-1}$ (Table I) all lower lying rotational levels have to be included in the computation.

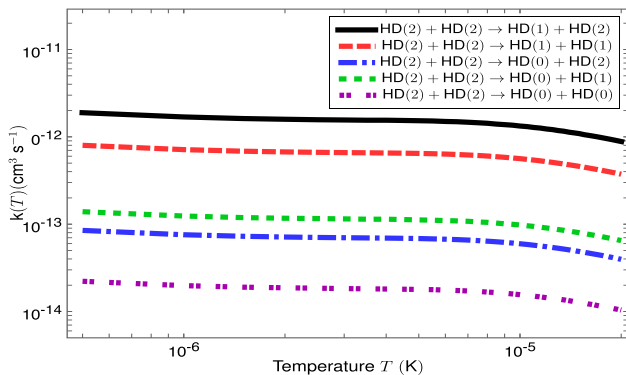


FIG. 9: (Color online) The same as in Fig. 6 for following processes: $\text{HD}(2) + \text{HD}(2) \rightarrow \text{HD}(1) + \text{HD}(2)$, $\text{HD}(2) + \text{HD}(2) \rightarrow \text{HD}(1) + \text{HD}(1)$, $\text{HD}(2) + \text{HD}(2) \rightarrow \text{HD}(0) + \text{HD}(2)$, $\text{HD}(2) + \text{HD}(2) \rightarrow \text{HD}(0) + \text{HD}(1)$, and $\text{HD}(2) + \text{HD}(2) \rightarrow \text{HD}(0) + \text{HD}(0)$.

It is known that a quantum-mechanical transition probability $P_{\alpha \rightarrow \beta}$ between any two quantum states, for example, the initial $\alpha = (j_1 j_2)$ and final $\beta = (j'_1 j'_2)$, is inversely proportional to the energy gap $\Delta \varepsilon_{\alpha \beta}$ between these two states. In turn, the cross sections $\sigma_{\alpha \beta}(E)$ and corresponding thermal rate coefficients $k_{\alpha \beta}(T)$ are directly proportional to the quantum probabilities. Thus

$$k_{\alpha \rightarrow \beta}(T) \sim 1/\Delta \varepsilon_{\alpha \beta}. \quad (10)$$

However, a quite unexpected result relating the rates in the following reactions is seen in the present study:



It is seen from Fig. 7, that process (11) has much larger thermal rate coefficients than process (12). The difference between these rates is about an order of magnitude. At the same time the energy difference between the HD molecule rotational states in (11) is $\Delta \varepsilon_{02-01} = 178.8 \text{ cm}^{-1}$, which is larger than in (12), for which $\Delta \varepsilon_{02-11} = 89.4 \text{ cm}^{-1}$. In accord with the relationship (10) one could expect that the process (11) would have lower values of the thermal rates than the process (12), but it does not. This happens because in (12) both HD molecules simultaneously change their internal states, i.e. rotational quantum numbers. Probably, this is the reason that the process (12) is much slower than (11). This result is somewhat similar to older computational data on the $\text{H}_2 + \text{H}_2$ collision [32, 43], where the authors found that the excitation process $\text{H}_2(0) + \text{H}_2(0) \rightarrow \text{H}_2(4) + \text{H}_2(2)$ has larger cross sections at larger collision energies than the process $\text{H}_2(0) + \text{H}_2(0) \rightarrow \text{H}_2(4) + \text{H}_2(0)$.

IV. CONCLUSIONS AND FUTURE WORK

Currently theoretical and experimental research in the field of the molecular Bose-Einstein condensates at ultracold temperatures is increasingly gaining momentum [1, 44, 45]. For example, in the recent work [45] the authors develop a promising approach for laser cooling of diatomic polar molecules. The method should allow the production of large samples of molecules at ultracold temperatures. Only a few of the possible practical and technological applications where new results of this research could be used have been briefly outlined in the Introduction. Researchers in this new field of atomic, molecular and optical physics have had tremendous success within last two decades. It is useful to have exact, high quality full space PESs for such polar molecule interactions. In turn the HD+HD system could be a prototype collision between two polar molecules with a high quality full space four-atomic PES. In this work we performed a detailed quantum-mechanical study of the state-resolved rotational excitation/de-excitation collisions between hydrogen molecules. The $\text{HD} + \text{HD} \rightarrow \text{HD} + \text{HD}$ and $\text{H}_2 + \text{H}_2 \rightarrow \text{H}_2 + \text{H}_2$ collisions have been considered and their rotational state-selected integral cross sections have been computed for a wide range of temperatures, i.e. from ultracold $T \sim 10^{-8} \text{ K}$ to up to $T \sim 14000 \text{ K}$. We have demonstrated that a small change in the H_2 - H_2 PES to adjust for HD-HD can lead to substantial differences in the scattering outputs, i.e. in the integral state resolved cross sections. This calculation was carried out within a single H_4 PES from Ref. [29].

Further, in connection with the problems of coherent control of the atomic and molecular interactions the authors of Ref. [46] performed a numerical investigation of the quantum entanglement for the case of a non-reactive ultracold collision between two indistinguishable ($\text{H}_2 + \text{H}_2$) molecules. Similarly, the initial state quantum entanglement coupling has been considered for the case of ultracold collision between identical two-atomic polar molecules [47]. It would also be useful to mention here that universal relations for strongly correlated fermions have been derived recently [48, 49]. Because the HD molecules are fermions with a well known interaction potential, they could be useful, for example, in direct numerical verification of these universal relations.

The authors of Ref. [50] formulated a time-independent quantum-mechanical formalism to describe the dynamics of molecules with permanent electric dipole moments in a two-dimensional confined geometry such as in a one-dimensional optical lattice. It would be useful in future investigation to adopt these techniques and apply them to a fermionic molecule system such as HD+HD with a well-known potential [29, 51]. It would be interesting to see differences in the quantum dynamics between the state-resolved HD+HD rotational thermal rate coefficients of the current work and possible new thermal rates for the same system but when embedded in a one-dimensional optical lattice or a microwave trap.

Acknowledgments

CNPq and FAPESP of Brazil.

This work was partially supported by Office of Sponsored Programs (OSP) of St. Cloud State University, and

-
- [1] K. -K. Ni *et al.*, *Science* **322**, 231 (2008).
 [2] D. DeMille, *Phys. Rev. Lett.* **88**, 067901 (2002).
 [3] P. Rabl, D. DeMille, J. M. Doyle, M. D. Lukin, R. J. Schoelkopf, and P. Zoller, *Phys. Rev. Lett.* **97**, 033003 (2006).
 [4] E.R. Hudson, N. B. Gilfoy, S. Kotochigova, J. M. Sage, and D. DeMille, *Phys. Rev. Lett.* **100**, 203201 (2008).
 [5] D. Herschbach, *Faraday Discuss.* **142**, 9 (2009).
 [6] M. T. Bell and T. P. Softley, *Mol. Phys.* **107**, 99 (2009).
 [7] P. Zoller *et al.*, *Eur. Phys. J. D* **36**, 203 (2005).
 [8] K. Hammerer, A.S. Sorensen, and E.S. Polzik, *Rev. Mod. Phys.* **82**, 1041 (2010).
 [9] K. Mishima and K. Yamashita, *Chem. Phys.* **379**, 13 (2011); *J. Chem. Phys.* **131**, 014109 (2009).
 [10] A. V. Gorshkov, S. R. Manmana, G. Chen, J. Ye, E. Demler, M. D. Lukin, and A. M. Rey, *Phys. Rev. Lett.* **107**, 115301 (2011).
 [11] J.M. Hutson and P. Soldan, *Int. Rev. Phys. Chem.* **26**, 1 (2007).
 [12] T.-G. Lee, N. Balakrishnan, R. C. Forrey, P. C. Stancil, D. R. Schultz, and G. J. Ferland, *J. Chem. Phys.* **125**, 114302 (2006); **126**, 179901 (2007).
 [13] R. V. Krems, *Phys. Chem. Chem. Phys.* **10**, 4079 (2008).
 [14] B. C. Sawyer, B. K. Stuhl, D. Wang, M. Yeo, and J. Ye, *Phys. Rev. Lett.* **101**, 203203 (2008).
 [15] V. Roudnev and M. Cavagnero, *Phys. Rev. A* **79**, 014701 (2009).
 [16] R. A. Sultanov, D. Guster, and S. K. Adhikari, arXiv:1111.2599.
 [17] K. -K. Ni *et al.*, *Nature (London)* **464**, 1324 (2010).
 [18] K.-K. Ni, S. Ospelkaus, D. J. Nesbitt, J. Ye and D. S. Jin, *Phys. Chem. Chem. Phys.*, **11** (42), 9626 (2009).
 [19] W.R. Gentry and C.F. Giese, *Phys. Rev. Lett.* **39**, 1259 (1977).
 [20] D.L. Johnson, R.S. Grace, and J. G. Skofronick, *J. Chem. Phys.* **71**, 4554 (1979).
 [21] D.W. Chandler and R. L. Farrow, *J. Chem. Phys.* **85**, 810 (1986).
 [22] R.L. Farrow and D.W. Chandler, *J. Chem. Phys.* **89**, 1994 (1988).
 [23] K. Takayanagi, *Sci. Rep. Saitama Univ. A3*, No. 2, **87** (1959).
 [24] A. Gelb and J.S. Alper, *Chem. Phys.* **39**, 141 (1979).
 [25] M. Cacciatore and G. D. Billing, *J. Phys. Chem.* **96**, 217 (1992).
 [26] T. Kusakabe, L. Pichl, R. J. Buenker, M. Kimura, and H. Tawara, *Phys. Rev. A* **70**, 052710 (2004).
 [27] S. Green, *J. Chem. Phys.* **62**, 2271 (1975); **67**, 715 (1977).
 [28] T. G. Heil, S. Green, and D. J. Kouri, *J. Chem. Phys.* **68**, 2562 (1978).
 [29] A.I. Boothroyd, P.G. Martin, W.J. Keogh, and M.J. Peterston, *J. Chem. Phys.*, **116**, 666 (2002).
 [30] J. Schaefer, *Astron. Astrophys. Suppl. Ser.* **85**, 1101 (1990).
 [31] D.R. Flower, *Mont. Not. R. Astron. Soc.* **297**, 334 (1998).
 [32] R. A. Sultanov and D. Guster, *Chem. Phys.* **326**, 641 (2006).
 [33] R. A. Sultanov, S.K. Adhikari, and D. Guster, *Phys. Rev. A* **81**, 022705 (2010).
 [34] J.M. Hutson, S. Green, Molscat ver. 14, Distributed by Collabor. Comp. Proj. 6, Daresbury Lab., UK, Eng. Phys. Sci. Res. Council, 1994.
 [35] P. Diep and J. K. Johnson, *J. Chem. Phys.* **112**, 4465 (2000); **113**, 3480 (2000).
 [36] M. Born and R. Oppenheimer, *Ann. Phys.* **84**, 457 (1927).
 [37] G. Danby, D.R. Flower, and T.S. Monteiro, *Mon. Not. R. Astr. Soc.* **226**, 739 (1987).
 [38] L. Monchick and J. Schaefer, *J. Chem. Phys.* **73**, 6153 (1980).
 [39] R. A. Sultanov and D. Guster, *Chem. Phys. Lett.* **428**, 227 (2006).
 [40] B. Mate, F. Thibault, G. Tejada, J.M. Fernandez, and S. Montero, *J. Chem. Phys.* **122**, 064313 (2005).
 [41] R. A. Sultanov and D. Guster, *Chem. Phys. Lett.* **436**, 19 (2007).
 [42] R. A. Sultanov, A. V. Khugaev, and D. Guster, *Chem. Phys. Lett.* **475**, 175 (2009).
 [43] F. Gatti, F. Otto, S. Sukiasyan, and H.-D. Meyer, *J. Chem. Phys.* **123**, 174311 (2005).
 [44] D. S. Jin and J. Ye, *Physics Today*, May 2011, 27.
 [45] E.S. Shuman, J.F. Barry, and D. DeMille, *Nature (London)* **467**, 820 (2010).
 [46] J. Gong, M. Shapiro, and P. Brumer, *J. Chem. Phys.* **118**, 2626 (2003).
 [47] R. A. Sultanov, D. Guster, and S. K. Adhikari, In: *Book of Abstracts: Int. Conf. on Quantum Information Processing and Communication (QIPC)*, Sep. 5-9, 2011, ETH, Zurich, Switzerland, p.123.
 [48] S. K. Adhikari, *J. Phys. B* **43**, 085304 (2010).
 [49] S. Tan, *Ann. Phys.* **323**, 2952 (2008); **323**, 2971 (2008); **323**, 2987 (2008).
 [50] G. Quemener and J.L. Bohn, *Phys. Rev. A* **81**, 060701(R) (2010); *A* **83**, 012705 (2011).
 [51] R. J. Hinde, *J. Chem. Phys.* **128**, 154308 (2008).